energy&fuels

Article

Cite This: Energy Fuels 2019, 33, 788−795

pubs.acs.org/EF

Methane (CH_4) Wettability of Clay-Coated Quartz at Reservoir Conditions

Bin Pan,[†] Franca Jones,[‡] Zhaoqin Huang,[§] Yongfei Yang,*[,§] Yajun Li,*[,∥] Seyed Hossein Hejazi,*[,†] and Stefan Iglauer*[,⊥]

[†]Department of Chemical and Petroleum Engineering, University of Calgary, Calgary T2N 1N4, Canada

[‡]Department of Chemistry, Nanochemistry Research Institute, Curtin University, P.O. Box U1987, Perth WA 6845, Australia

[§]School of Petroleum Engineering, China University of Petroleum (East China), No. 66, Changjiang West Road, Qingdao 266580, P.R. China

[∥]Key Laboratory of Unconventional Oil & Gas Development (China University of Petroleum (East China)), Ministry of Education, Qingdao 266580, P.R. China

[⊥]School of Engineering, Edith Cowan University, 270 Joondalup Drive, Joondalup WA 6027, Australia

Supporting Information

ABSTRACT: Methane (CH_4) wettability of shale is a key parameter which determines pore and reservoir-scale fluid distributions, CH_4 reserves estimation, and ultimate recovery efficiency from shale gas reservoirs. Clay minerals usually fill the pore spaces or are adsorbed on the surface of shale rock, thus influencing CH_4 wettability. However, a systematic investigation of the influence of clay on CH_4 shale wettability is lacking. Herein, we investigated the role of clay, pressure, temperature, and salinity on CH_4 wettability of clay-coated quartz (i.e., a well-defined model system for shales). Results indicated that the advancing and receding water contact angles for clean, kaolinite-coated, and montmorillonite-coated quartz increased with pressure. However, the effect of temperature on wettability is complex, and thus the advancing water contact angle for clean quartz increased with temperature while an opposite trend was found for clay-coated quartz. At low temperature (i.e., 300 K), clay coating dewetted the quartz surface, while at elevated temperature (i.e., 323 K), clay coating increased the hydrophilicity of the quartz surface. Furthermore, kaolinite clay particles demonstrated a stronger influence on quartz wettability than montmorillonite particles, both at high and low temperatures. In addition, higher NaCl salinity led to higher advancing water contact angles for the aforementioned three solid surfaces. The effect of salinity on CH_4 wettability is thus intensified in the presence of clays. These insights will thus improve the accuracy of CH_4 reserve estimates and aid methane recovery schemes.

1. INTRODUCTION

Shale reserves play an important role in meeting the global demands for energy. The significant development in gas production from such shale gas reservoirs is due to advances in horizontal drilling and hydraulic fracturing technology.[1−6] However, in commercial production, there are challenges in evaluating the characteristics of these hydrocarbon reservoirs due to the complexity of gas storage and transport processes in the micro- and nanoscale pore geometries.[7,8] In this context, wettability, characterized by the brine contact angles of CH_4−brine−shale rock (θ) is a key parameter that determines CH_4 reserves and production efficiency.[9−13] In particular, CH_4 reserves, CH_4 distribution, and free gas flow in the shale pores are strongly affected by the capillary pressure (P_c) which is a function of contact angle.[12,14−22] For example, for a circular capillary tube, capillary pressure can be calculated based on the Young−Laplace equation:

$$P_c = \frac{2\gamma \cos\theta}{r} \quad (1)$$

where γ is the interfacial tension between CH_4 and brine and r is the average pore radius. When $\theta < 90°$, the shale rock has a stronger affinity to brine than CH_4 and P_c could be a driving force for CH_4 recovery as water would imbibe more easily; while if $\theta > 90°$, the shale rock is more CH_4-wet than water-wet and P_c would tend to resist water imbibition.

Organic rich shales are mainly composed of consolidated clay-sized particles with a high organic content, a complex chemical composition that is filled or covered with clay,[23−25] which complicates contact angle analysis. For example, the clay crystal size is much smaller than the usual sessile droplet, which prevents standard wettability measurements.[26−28] Previous literature reports that kaolinite and montmorillonite crystal sizes are smaller than 2 μm,[29,30] while the usual sessile droplet size is around 2000 μm.[31,32] To avoid the challenge to measure the contact angle of clay using the sessile method, Borysenko et al. used a liquid−liquid extraction method to validate montmorillonite as a hydrophilic surface and kaolinite as a hydrophobic surface.[28] However, the liquid−liquid extraction method could not report the specific contact angle value.[33] Schmatz et al. reported a more water-wet nature of kaolinite based on cryo SEM results.[34] However, the cryo SEM method is destructive.[35] Ballah et al. measured the wettability of clay coating on a glass slide using the sessile method, and all

Received: October 9, 2018
Revised: January 17, 2019
Published: January 17, 2019

Downloaded via UNIV OF MANCHESTER on May 17, 2023 at 22:45:47 (UTC).
See https://pubs.acs.org/sharingguidelines for options on how to legitimately share published articles.

© 2019 American Chemical Society

DOI: 10.1021/acs.energyfuels.8b03536
Energy Fuels 2019, 33, 788−795

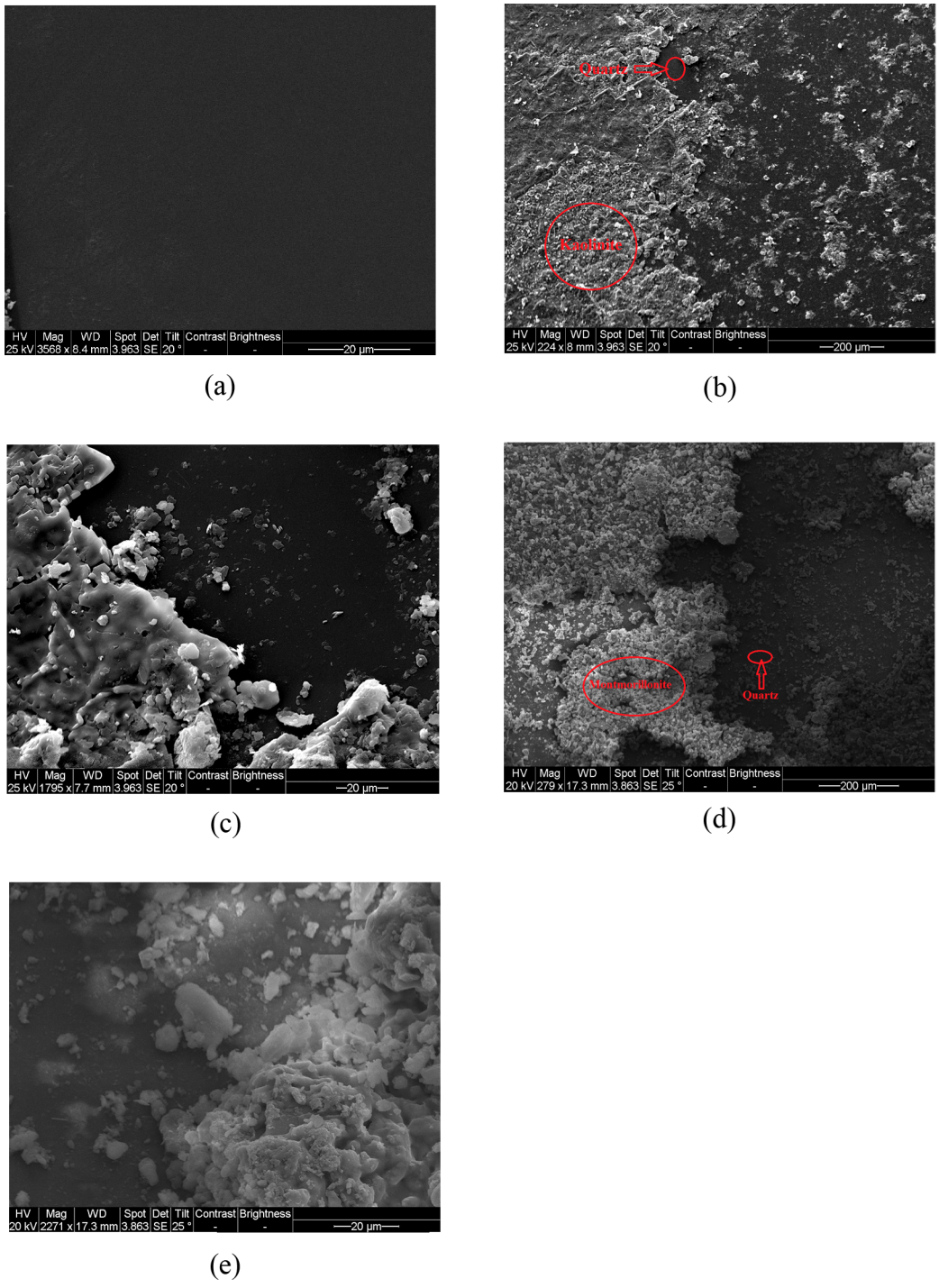

Figure 1. SEM images of clean (a), kaolinite-coated (b, c), and montmorillonite-coated (d, e) quartz used in the experiments. The light color is clay particles and the dark color is quartz substrate.

the contact angles measured in their work were smaller than 40° (i.e., a strong water-wet surface).[36] However, all their measurements were conducted at ambient conditions, which could not represent the real wettability of clay at reservoir conditions as pressure and temperature could also influence wettability significantly.[37,38] A recent study compacted clay powders into solid substrates and measured the brine contact angles of the CO_2/N_2/oil−brine−clay systems at reservoir conditions.[39] They concluded that montmorillonite is oil-wet, while kaolinite and illite are water-wet at typical reservoir conditions.[39] However, they did not measure clay wettability in the CH_4−brine−clay system, which is related to shale gas production.[9−13] Molecular dynamic simulations, which overcome these limitations, predicted that Na-/Ca-montmorillonite becomes more hydrophobic when exposed to CO_2 at reservoir conditions.[40] Šolc et al. calculated the contact angle of water−air−kaolinite was 105° using molecular dynamic simulation.[41] Thus, the inconsistency between experimental and simulated results is clear and clay wettability is still open to large uncertainty. However, how clay influences the wettability of organic rich shales at reservoir conditions has not been explored.

DOI: 10.1021/acs.energyfuels.8b03536
Energy Fuels 2019, 33, 788−795

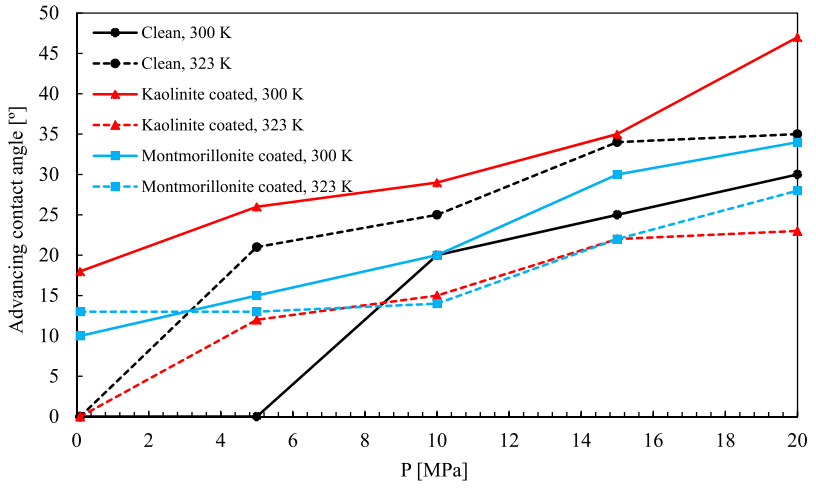

(a)

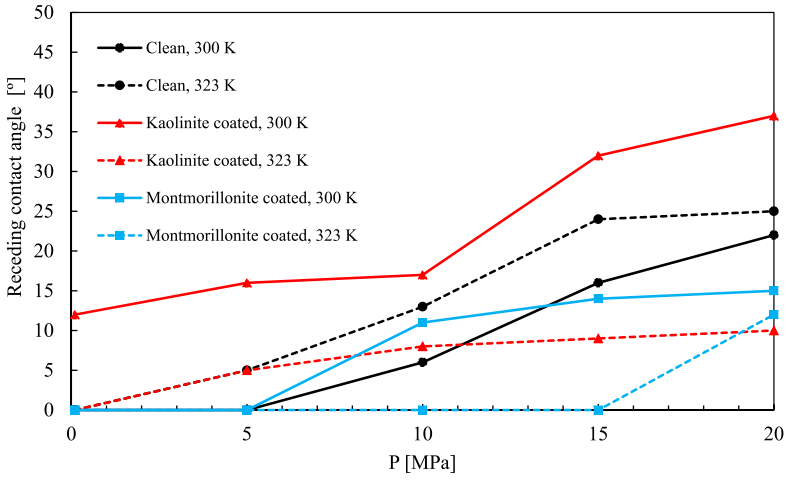

(b)

Figure 2. Effect of pressure and temperature on the (a) advancing and (b) receding brine contact angles of clean/kaolinite-coated/montmorillonite-coated quartz−CH_4−brine systems. Note that the aqueous phase is 1.5 wt % NaCl brine.

In the present study, we thus investigate the CH_4 wettability of clay-coated quartz at reservoir conditions. Note that we use the words clay and clay minerals interchangeably in this work. To isolate the role of shale constituents, we use quartz, one of the most primary components of shale,[42−47] coated with clay particles, instead of real rock samples. Thus, we can elucidate the role of clay types on the wettability without perturbations from other chemical components in shale. Furthermore, the effects of pressure, temperature, and salinity on CH_4 wettability are also presented.

2. EXPERIMENTAL METHODOLOGY

To remove any residual contaminants from the quartz surface,[48,49] all alpha-quartz substrates (supplied by Dade Quartz Co., Ltd., China, with RMS surface roughness of less than 1 nm measured with an JPK NanoWizard 4 atomic force microscope (AFM), Figure S1a) were carefully cleaned following a standard procedure. First, the substrates were washed by acetone and subsequently soaked in piranha solution (3 parts of 98 wt % H_2SO_4 and 1 part of aqueous 30 wt % H_2O_2 for 30 min at 300 K; H_2SO_4 and H_2O_2 were purchased from Sinopharm Chemical Reagent Co., Ltd.). Afterward, the immersed substrates were covered with aluminum foil and dried in a clean oven for 8 h at 353 K. A concentration of 2 wt % kaolinite or montmorillonite suspension was prepared respectively through adding kaolinite or montmorillonite powders into 1.5 wt % NaCl brine (kaolinite, montmorillonite, and sodium chloride were obtained from Sigma-Aldrich; NaCl purity was ≥99 mol %). Note that the chemical formula of kaolinite is $Al_2O_7Si_2{\cdot}2H_2O$ and the montmorillonite is a K 10 catalyst, $MgNaAl_5(Si_4O_{10})_3(OH)_6$. A relatively high NaCl salinity was used here to impede clay accumulation/swelling and promote clay adsorption onto the quartz surface.[50,51] The total salinities of clay suspensions in DI water and in 1.5 wt % NaCl brine were measured using Starter3100 M at room temperature (see Table S1). It was found that the total salinity of clay suspensions is extremely low, showing no apparent difference with the salinity of pure DI water. A concern may be that such a high Na^+ concentration would exchange with in situ divalent cations from clay minerals. However, as we show in Tables S1 and S2, the ion salinities from in situ clay were extremely low and the wettabilities for Na^+ and Mg^{2+} were very similar. Thus, it was assumed that the ion exchange would not influence wettability in this work. The particle size distributions (PSD) of the kaolinite and montmorillonite were measured thrice via a Zetasizer Nano instrument (Malvern, U.K.). The average particle sizes for kaolinite and montmorillonite were 1050 and 900 nm, respectively. The total organic content (TOC) for kaolinite and montmorillonite were 335 and 3093 mg/kg, respectively, measured by an Elab-TOC instrument.

DOI: 10.1021/acs.energyfuels.8b03536
Energy Fuels 2019, 33, 788−795

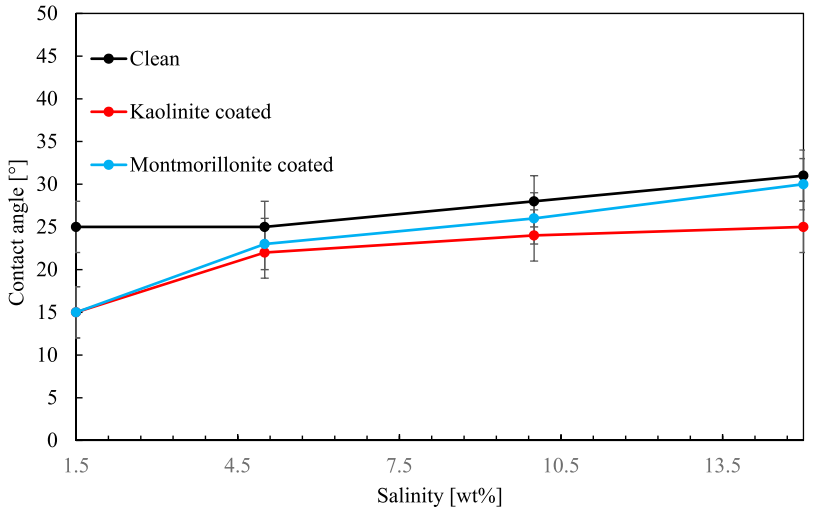

Figure 3. Advancing brine contact angles of CH_4–clean/kaolinite-coated/montmorillonite-coated quartz–brine systems at 10 MPa and 323 K.

The kaolinite and montmorillonite suspensions were stirred for 2 h at 323 K. Afterward, the clean quartz substrates were aged in the 2 wt % kaolinite or montmorillonite suspensions for 6 h, and then the aged substrates were covered with clean aluminum foil and dried for 6 h. The total 12 h duration would ensure a stable coating.[50] The morphological properties of clean and coated substrates were characterized using AFM (note that RMS roughness values of clean and kaolinite-coated quartz were measured by a JPK NanoWizard 4 atomic force microscope, while RMS of montmorillonite quartz was measured via a Bruker Multi Mode 8 atomic force microscope, please see Figure S1) and SEM measurements by a Philips XL 30 SEM (Figure 1). The RMS roughness values for clean, kaolinite-coated, and montmorillonite-coated quartz were 483.7 pm, 629.8 nm, and 863 nm, respectively. However, at this scale, the effect of roughness on contact angle is insignificant.[52] Based on the analysis of SEM images using MATLAB, the average kaolinite and montmorillonite coverages were 37.48% and 39.02%, respectively (see Figure S2). Furthermore, the SEM images demonstrated a more compact coating on the montmorillonite-coated surface. The advancing (θ_a) and receding (θ_r) brine contact angles of CH_4–brine–clean/clay-coated quartz systems were then measured by a Krüss DSA 100 instrument using the tilted plate method[53] as described previously in detail.[23] All the contact angle measurements were finished within the initial 30 s. We did not observe the contact angle for a long time in this work, because the droplet could destabilize and displace the clay coating after long time contact. However, a future work would investigate long-term clay wettability using a recent developed LbL coating method.[54] Furthermore, we did not consider the influence from CH_4–brine dissolution because of a very low dissolution capacity between brine and CH_4.[55] Note that in shale gas extraction, θ_a corresponds to CH_4 recovery, while θ_r is related to initial CH_4/water distribution.[56]

3. RESULTS AND DISCUSSION

3.1. Effect of Pressure and Temperature on Contact Angles. The effects of pressure and temperature on the brine contact angles were measured for the various substrates at multiple pressures (0.1 to 20 MPa) and temperatures (300 and 323 K), see Figure 2.

Both θ_a and θ_r for all substrates clearly increased with pressure, consistent with literature data measured for several different gases on various substrates.[23,38,43,52,57−59] For example, at 300 K, when pressure increased from 0.1 to 20 MPa, θ_a for clean, kaolinite-coated, and montmorillonite-coated quartz increased by 30°, 29°, and 21°, respectively, while θ_r for the above three surfaces increased by 22°, 25°, and 15°, respectively.

Noteworthy was the effect of temperature on the wettability. θ_a for clean quartz increased with temperature, consistent with literature data reported for quartz,[52] hydrophilic dolomite,[31] and shale,[37] while θ_a for clay-coated quartz decreased with temperature, consistent with literature data reported for mica,[58,59] hydrophobic dolomite,[31] and 3 wt % TOC shale.[23] Specifically, at 15 MPa, when temperature increased from 300 to 323 K, θ_a changes for clean, kaolinite-coated, and montmorillonite-coated quartz were 9°, −13°, and −8°, respectively; at 20 MPa, for the same temperature increase, θ_a changes for the above three surfaces were 5°, −24°, and −6°, respectively.

Physically, the influence of pressure on wettability can be attributed to the higher nonaqueous phase density,[38,57] the consequently stronger intermolecular interactions between CH_4 and the solid surface due to the increased molecular density,[23,57,60−63] and the corresponding decrease in the interfacial tension between the solid surface and CH_4.[64] The underlying mechanism of the temperature influence on wettability can be explained by the sharp-kink approximation,[31,37] as shown in eq 2 below.

$$\cos\theta = -1 + \frac{\Delta\rho I}{\gamma_{lg}} \tag{2}$$

where $\Delta\rho$ is the approximate density difference between the adsorbed brine film and CH_4, γ_{lg} is the interfacial tension between brine and CH_4, and I is the van der Waals potential integral.

Clearly, both γ_{lg} and $\Delta\rho$ increased with temperature.[58,65] However, the relative increase in $\Delta\rho$ with temperature was more significant than that of γ_{lg},[31,37] which reduces the contact angle; the van der Waals potential decreases with temperature,[66] which increases the contact angle. Thus, in both scenarios, a θ increase or decrease with temperature is possible. For clean quartz, the temperature-driven influence on van der Waals interaction was more effective, resulting in a contact angle increase with temperature.[31] For clay-coated quartz, this van der Waals interaction might be relatively weak, and thus the contact angle decreased with temperature.

3.2. Effect of Brine Salinity on Contact Angles. All θ_a increased with salinity as depicted in Figure 3. Specifically, when NaCl salinity increased from 1.5 to 15 wt %, θ_a for clean,

DOI: 10.1021/acs.energyfuels.8b03536
Energy Fuels 2019, 33, 788−795

Table 1. Zeta Potential and pH Data for Various Systems at Two Different Temperatures in This Work

sample	T (K)	mean zeta potential (mV)	standard deviation (mV)	mean pH	standard deviation
1.5 wt % NaCl	300	−0.86	1.01	6.45	
1.5 wt % NaCl	323	1.21	0.786		
5 wt % NaCl	300	1.91	4.94	6.25	0.03
5 wt % NaCl	323	3.49	6.65		
2 wt % kaolinite + 1.5 wt % NaCl	300	−14.7	0.436	6.25	0.58
2 wt % montmorillonite + 1.5 wt % NaCl	300	−21.9	0.574	4.74	0.23
2 wt % kaolinite + 1.5 wt % NaCl	323	−12.6	0.872		
2 wt % montmorillonite + 1.5 wt % NaCl	323	−19.6	0.967		
2 wt % kaolinite + 5 wt % NaCl	300	−7.51	7.88	5.61	0.02
2 wt % montmorillonite + 5 wt % NaCl	300	−10.1	6.3	3.48	0.01
2 wt % kaolinite + 5 wt % NaCl	323	−3.04	6.58		
2 wt % montmorillonite + 5 wt % NaCl	323	−2.14	3.59		
2 wt % kaolinite + 10 wt % NaCl	323	2.37	9.31		
2 wt % montmorillonite + 10 wt % NaCl	323	3.48	8.97		

kaolinite-coated, and montmorillonite-coated quartz increased by 6°, 15°, and 10°, respectively.

This result is consistent with literature data for NaCl−oil−sandstone,[67] NaCl−glass/kaolinite-coated glass−crude oil,[68] NaCl−oil−kaolinite-coated glass,[69] NaCl−CO_2−mica,[58,59,70] and NaCl−CO_2−quartz[38,62] systems. The effect of salinity on the advancing water contact angles can be explained with the Derjaguin−Landau−Verwey−Overbeek (DLVO) theory as discussed in our previous work.[23] In order to shed more light on the underlying mechanism of salinity influence on the contact angles, we also measured the corresponding zeta potentials (using a Zetasizer Nano instrument, Malvern, U.K.) and pH values (using a RHA-SHKY pH meter model 8601 instrument), see Table 1. Every zeta-potential measurement was repeated 18 times, and every pH measurement was repeated 3 times.

Higher temperatures led to less negative zeta potentials, while the addition of kaolinite or montmorillonite reduced the zeta potential. Furthermore, clay suspensions are not stable and uniform solutions, and this intrinsic property could cause a significant variation in the measured properties.[71]

In addition, montmorillonite suspensions were more acidic than the corresponding kaolinite suspensions, while a higher NaCl salinity led to a lower pH value for both montmorillonite and kaolinite suspensions. Higher pH values led to more negative zeta potentials[72] and thus lower contact angles. However, it could not be explained why the contact angle for 2 wt % montmorillonite + 1.5 (or 5) wt % NaCl brine sample was smaller than that for 2 wt % kaolinite + 1.5 (or 5) wt % NaCl brine sample at 300 K just based on pH. We hypothesize that the surface microstructural evolution and (clay) hydration of the coated surface also played an important role, causing the different wettability behaviors for kaolinite- and montmorillonite-coated surfaces, besides the solution property.[60,73] Clearly, the contact angle strongly correlated with the zeta potential, as shown in Table 2 and Figure 4.

At 323 K, a higher salinity led to a larger zeta potential, thus higher contact angles. The zeta potential for kaolinite was smaller than that for montmorillonite at the same NaCl salinity (5 and 10 wt %, respectively), and thus the contact angle for kaolinite was smaller than montmorillonite. However, note that the zeta potential was measured at ambient conditions, while the contact angle was measured at high pressure, although a correlation has been proposed previously.[71]

Table 2. Used Data for Plotting Figure 4

solution system	zeta potential (mV)	advancing contact angle (deg)
2 wt % montmorillonite + 1.5 wt % NaCl	−19.6	15
2 wt % kaolinite + 1.5 wt % NaCl	−12.6	15
2 wt % kaolinite + 5 wt % NaCl	−3.04	22
2 wt % montmorillonite + 5 wt % NaCl	−2.14	23
2 wt % kaolinite + 10 wt % NaCl	2.37	24
2 wt % montmorillonite + 10 wt % NaCl	3.48	26

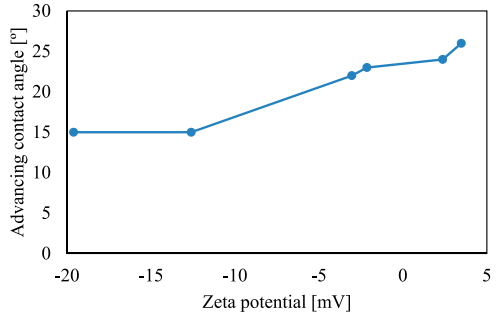

Figure 4. Relationship between advancing contact angle and the corresponding zeta potential at 10 MPa, 323 K, and various NaCl salinities.

In summary, the increasing salinity increases the ionic strength, which better screens the surface charge.[61] Thus, the surface potential approaches zero and, in some circumstances, positive values. As a result, surface polarity and water affinity decreases, and hence, an increasing water contact angle results.

3.3. Effect of Clay on Quartz Wettability. Based on the results and discussion in Sections 3.1and 3.2, it is easy to conclude that the effect of clay on quartz wettability is extremely complex. For example, the effect of clay coating on quartz wettability was different at low and high temperatures, see Figure 2. At low temperature (i.e., 300 K), kaolinite or montmorillonite coating dewetted the quartz, which could be attributed to the lowered pH and intensified acidic properties, thus less negative zeta potential,[72] and a larger contact angle,[74] while at high temperature (i.e., 323 K), these coatings intensified quartz hydrophilicity.

DOI: 10.1021/acs.energyfuels.8b03536
Energy Fuels 2019, 33, 788−795

Furthermore, kaolinite always had a stronger influence on quartz wettability than montmorillonite. For example, at 20 MPa and 300 K, θ_a values for clean, kaolinite-coated, and montmorillonite-coated quartz were 30°, 47°, and 34°, respectively, while at 20 MPa and 323 K, θ_a values for the above three surfaces were 35°, 23°, and 28°. The low temperature results (300 K) are consistent with literature reports that (a) kaolinite and montmorillonite clays were more oil-wet than quartz at 298 K and 0.1 MPa,[28] that (b) quartz had a stronger water adsorption capacity than kaolinite at 298 K,[75] and that (c) brine contact angles of oil−water−sandstone systems increased with clay content on the sandstone surface at ambient conditions (i.e., 0.1 MPa and 287 K).[67] Furthermore, the results for the clay influence at 323 K are consistent with literature reports where kaolinite reduced water repellency of silica sand at 323 K more efficiently than montmorillonite.[76] Although a recent study reported clay wettability for CO_2/N_2/oil−brine−clay systems at reservoir conditions,[39] we did not find any literature related to clay influence on shale wettability at high temperature and high pressure, noting that reservoir conditions (i.e., elevated pressure and temperature) are critical for gas behavior at the pore-scale,[77] which is again vital for the evaluation of CH_4 reserves and recovery.

In addition, the effect of salinity on CH_4 wettability was intensified in the presence of clays at 10 MPa and 323 K, see Figure 3. Specifically, when the NaCl salinity increased from 1.5 to 15 wt % for clean quartz, θ_a increased by 6° from 25° to 31°; compared with this, salinity had a stronger influence on θ_a for the kaolinite-coated (e.g., θ_a increased by 10° from 15° to 25°) and montmorillonite-coated (e.g., θ_a increased by 15° from 15° to 30°) surfaces. Mechanistically, clay particles have negatively charged surfaces at typical reservoir conditions,[78] consistent with our zeta-potential results; the isoelectric points for quartz, kaolinite, and montmorillonite are pH = 3,[52] 6, and 6.7.[78] Montmorillonite has a greater number of structurally charged sites than kaolinite,[79] which results in a stronger attraction to positive charges (e.g., Na^+). Thus, the surface potential for montmorillonite-coated quartz approaches zero more quickly. Consequently, θ_a for montmorillonite-coated quartz increased more significantly than θ_a for both kaolinite-coated quartz and clean quartz.

4. CONCLUSIONS

CH_4−shale wettability is a key parameter for predicting CH_4 reserves and distribution.[9−13] However, due to the complexity of the shale structure and composition, CH_4−shale wettability evaluation is still open to uncertainties. Specifically, clay minerals, as one of the abundant constituents of shale formations, significantly increase the complexity of CH_4−shale wettability. Furthermore, a systematic investigation of clay effects on CH_4−shale wettability in a representative system is still scarce. To elucidate how clay influences shale wettability, we used a well-defined model (i.e., clay-coated quartz) to investigate the role of clay, pressure, temperature, and salinity on the CH_4 wettability. The following conclusions were reached:

(1) The quartz substrates became more water-wet at high temperature (i.e., 323 K) when coated by clays, while they became more CH_4-wet at low temperatures (i.e., 300 K). Kaolinite had a stronger influence on quartz wettability than montmorillonite with respect to temperature variations. We did not find any previous reports to compare the influence of clay coating or adsorption on shale and quartz wettability at different temperatures, especially at reservoir pressures.

(2) Elevated pressures increased the hydrophobicity of all three tested surfaces (i.e., clean, kaolinite-coated, and montmorillonite-coated quartz).

(3) Elevated temperatures dewetted the clean quartz, while they increased the hydrophilicity of clay-coated quartz.

(4) High NaCl salinity reduced surface hydrophilicity. This salinity effect was intensified in the presence of clays.

■ ASSOCIATED CONTENT

Supporting Information

The Supporting Information is available free of charge on the ACS Publications website at DOI: 10.1021/acs.energyfuels.8b03536.

Atomic force microscopy images of clean, kaolinite-coated, and montmorillonite-coated quartz; random three areas of original and binary SEM images of kaolinte and montmorillonite coating; the total salinities of clay suspensions in DI water and 1.5 wt % NaCl brine at room temperature; and advancing contact angles for various systems at 10 MPa and 50 °C (PDF)

■ AUTHOR INFORMATION

Corresponding Authors

*E-mail: yangyongfei@upc.edu.cn (Y.Y.).
*E-mail: liyajun@upc.edu.cn (Y.L.).
*E-mail: shhejazi@ucalgary.ca (S.H.H.).
*E-mail: s.iglauer@ecu.edu.au (S.I).

ORCID

Bin Pan: 0000-0003-3482-5660
Franca Jones: 0000-0002-8461-8291

Notes

The authors declare no competing financial interest.

■ ACKNOWLEDGMENTS

The authors wish to acknowledge financial assistance from the National Science and Technology Major Project (2016ZX05023-001, 2016ZX05060-010, 2017ZX05009001), the Natural Science Foundation of China (41602143, 51774310, 51509260, 51674280, 51711530131), the Key Research and Development Plan of Shandong Province (2018GSF116009), the Applied Basic Research Projects of Qingdao Innovation Plan (16-5-1-38-jch), the Fundamental Research Funds for the Central Universities (18CX02104A, 18CX05029A, 17CX05003), the Chinese Scholarship Council, the University of Calgary Global Research Initiative in Unconventional Hydrocarbon Resources-Beijing Site, the Kerui-MITACS Accelerate Research Fund Application (IT09328), and the Natural Sciences and Engineering Research Council of Canada (NSERC).

■ REFERENCES

(1) Gregory, K. B.; Vidic, R. D.; Dzombak, D. A. Water management challenges associated with the production of shale gas by hydraulic fracturing. *Elements* **2011**, *7* (3), 181−186.
(2) Jarvie, D. M.; Hill, R. J.; Ruble, T. E.; Pollastro, R. M. Unconventional shale-gas systems: The Mississippian Barnett Shale of north-central Texas as one model for thermogenic shale-gas assessment. *AAPG Bull.* **2007**, *91* (4), 475−499.

DOI: 10.1021/acs.energyfuels.8b03536
Energy Fuels 2019, 33, 788−795

(3) Wang, J. J.; Wang, B. E.; Li, Y. J.; Yang, Z. H.; Gong, H. J.; Dong, M. Z. Measurement of dynamic adsorption−diffusion process of methane in shale. *Fuel* **2016**, *172*, 37−48.
(4) Aljamaan, H.; Al Ismail, M.; Kovscek, A. R. Experimental investigation and Grand Canonical Monte Carlo simulation of gas shale adsorption from the macro to the nano. *J. Nat. Gas Sci. Eng.* **2017**, *48*, 119−137.
(5) Dehghanpour, H.; Lan, Q.; Saeed, Y.; Fei, H.; Qi, Z. Spontaneous imbibition of brine and oil in gas shales: Effect of water adsorption and resulting microfractures. *Energy Fuels* **2013**, *27* (6), 3039−3049.
(6) Jiménez-Martínez, J.; Porter, M. L.; Hyman, J. D.; Carey, J. W.; Viswanathan, H. S. Mixing in a three-phase system: Enhanced production of oil-wet reservoirs by CO_2 injection. *Geophys. Res. Lett.* **2016**, *43*, 196−205.
(7) Curtis, M. E.; Sondergeld, C. H.; Ambrose, R. J.; Rai, C. S. Microstructural investigation of gas shales in two and three dimensions using nanometer-scale resolution imaging. *AAPG Bull.* **2012**, *96* (4), 665−677.
(8) Ambrose, R. J.; Hartman, R. C.; Diaz-Campos, M.; Akkutlu, I. Y.; Sondergeld, C. H. Shale gas-in-place calculations part I: New pore-scale considerations. *SPE Journal* **2012**, *17*, 219.
(9) Amann-Hildenbrand, A.; Ghanizadeh, A.; Krooss, B. M. Transport properties of unconventional gas systems. *Mar. Pet. Geol.* **2012**, *31* (1), 90−99.
(10) Takahashi, S.; Kovscek, A. R. Wettability estimation of low-permeability, siliceous shale using surface force. *J. Pet. Sci. Eng.* **2010**, *75* (1-2), 33−43.
(11) Chalmers, G. R. L.; Ross, D. J. K.; Bustin, R. M. Geological controls on matrix permeability of Devonian Gas Shales in the Horn River and Liard basins, northeastern British Columbia, Canada. *Int. J. Coal Geol.* **2012**, *103*, 120−131.
(12) Bai, B. J.; Elgmati, M.; Zhang, H.; Wei, M. Z. Rock characterization of Fayetteville shale gas plays. *Fuel* **2013**, *105*, 645−652.
(13) Sahimi, M. *Flow and transport in porous media and fractured rock: From conventional methods to modern approaches* **2011**, DOI: 10.1002/9783527636693.
(14) Hu, Y. N.; Devegowda, D.; Striolo, A.; Phan, A.; Ho, T. A.; Civan, F.; Sigal, R. F. Microscopic dynamics of water and hydrocarbon in shale-kerogen pores of potentially mixed wettability. *SPE Journal* **2014**, *20*, 112.
(15) Hui, S.; Xiaorong, L.; Xing, L.; Naigui, L.; Yukai, Q.; Tao, F.; Likuan, Z.; Yuhong, L. Effects of mix-wet porous mediums on gas flowing and one mechanism for gas migration. *J. Pet. Sci. Eng.* **2017**, *152*, 60−66.
(16) Nelson, P. H. Pore-throat sizes in sandstones, siltstones, and shales: Reply. *AAPG Bull.* **2011**, *95* (8), 1448−1453.
(17) Liang, L. X.; Luo, D. X.; Liu, X. J.; Xiong, J. Experimental study on the wettability and adsorption characteristics of Longmaxi Formation shale in the Sichuan Basin, China. *J. Nat. Gas Sci. Eng.* **2016**, *33*, 1107−1118.
(18) Zhou, Y. F.; Helland, J.; Hatzignatiou, D. G. A dimensionless capillary pressure function for imbibition derived from pore-scale modelling in mixed-wet-rock images. *SPE Journal* **2013**, *18*, 296.
(19) Zhou, Y. F.; Helland, J.; Jettestuen, E. Dynamic capillary pressure curves from pore-scale modelling in mixed-wet-rock images. *SPE Journal* **2013**, *18*, 634.
(20) Zhou, Y. F.; Helland, J.; Hatzignatiou, D. G. Pore-scale modelling of waterflooding in mixed-wet-rock images: Effects of initial saturation and wettability. *SPE Journal* **2014**, *19*, 88.
(21) Nielsen, L. C.; Bourg, I. C.; Sposito, G. Predicting CO_2−water interfacial tension under pressure and temperature conditions of geologic CO_2 storage. *Geochim. Cosmochim. Acta* **2012**, *81*, 28−38.
(22) Zhang, L. J.; Kim, Y. M.; Jung, H.; Wan, J. M.; Jun, Y. S. Effects of salinity-induced chemical reactions on biotite wettability changes under geologic CO_2 sequestration conditions. *Environ. Sci. Technol. Lett.* **2016**, *3* (3), 92−97.
(23) Pan, B.; Li, Y. J.; Wang, H. Q.; Jones, F.; Iglauer, S. CO_2 and CH_4 wettabilities of organic-rich shale. *Energy Fuels* **2018**, *32* (2), 1914−1922.
(24) Kuila, U.; Prasad, M. Specific surface area and pore-size distribution in clays and shales. *Geophys. Prospect.* **2013**, *61* (2), 341−362.
(25) Ross, D. J. K.; Marc Bustin, R. The importance of shale composition and pore structure upon gas storage potential of shale gas reservoirs. *Mar. Pet. Geol.* **2009**, *26* (6), 916−927.
(26) Iglauer, S.; Pentland, C. H.; Busch, A. CO_2 wettability of seal and reservoir rocks and the implications for carbon geo-sequestration. *Water Resour. Res.* **2015**, *51* (1), 729−774.
(27) Siddiqui, M. A. Q.; Ali, S.; Fei, H. X.; Roshan, H. Current understanding of shale wettability: A review on contact angle measurements. *Earth-Sci. Rev.* **2018**, *181*, 1−11.
(28) Borysenko, A.; Clennell, B.; Sedev, R.; Burgar, L.; Ralston, J.; Raven, M.; Dewhurst, D.; Liu, K. Y. Experimental investigations of the wettability of clays and shales. *J. Geophys. Res.* **2009**, *114* (B7), 1.
(29) Pir Cakmak, F.; Keating, C. D. Combining catalytic microparticles with droplets formed by phase coexistence: Adsorption and activity of natural clays at th activity of natural clays at the aqueous/Aqueous interface. *Sci. Rep.* **2017**, *7*, 3215.
(30) Innocent, C.; Fagel, N.; Hillaire-Marcel, C. Sm-Nd isotope systematics in deep-sea sediments: clay-size versus coarser fractions. *Mar. Geol.* **2000**, *168*, 79−87.
(31) Al-Yaseri, A. Z.; Roshan, H.; Zhang, Y.; Rahman, T.; Lebedev, M.; Barifcani, A.; Iglauer, S. Effect of the temperature on CO_2/brine/dolomite wettability: Hydrophilic versus hydrophobic surfaces. *Energy Fuels* **2017**, *31*, 6329−6333.
(32) Alnili, F.; Al-Yaseri, A.; Roshan, H.; Rahman, T.; Verall; Lebedev, M.; Sarmadivaleh, M.; Iglauer, S.; Barifcani, A. Carbon dioxide/brine wettability of porous sandstone versus solidquartz: An experimental and theoretical investigation. *J. Colloid Interface Sci.* **2018**, *524*, 188−194.
(33) Fuerstenau, D. W.; Diao, J. L.; Williams, M. C. Characterization of the wettability of solid particles by film flotation 1. Experimental investigation. *Colloids Surf.* **1991**, *60*, 127−144.
(34) Schmatz, J.; Urai, J. L.; Berg, S.; Ott, H. Nanoscale imaging of pore-scale fluid-fluid-solid contacts in sandstone. *Geophys. Res. Lett.* **2015**, *42* (7), 2189−2195.
(35) Alhammadi, A. M.; AlRatrout, A.; Singh, K.; Bijeljic, B.; Blunt, M. J. In situ characterization of mixed wettability in a reservoir rock at subsurface conditions. *Sci. Rep.* **2017**, *7*, 10753.
(36) Ballah, J.; Chamerois, M.; Durand-Vidal, S.; Malikova, N.; Levitz, P.; Michot, L. J. Effect of chemical and geometrical parameters influencing the wettability of smectite clay films. *Colloids Surf., A* **2016**, *511*, 255−263.
(37) Roshan, H.; Al-Yaseri, A. Z.; Sarmadivaleh, M.; Iglauer, S. On wettability of shale rocks. *J. Colloid Interface Sci.* **2016**, *475*, 104−111.
(38) Al-Yaseri, A. Z.; Roshan, H.; Lebedev, M.; Barifcani, A.; Iglauer, S. Dependence of quartz wettability on fluid density. *Geophys. Res. Lett.* **2016**, *43*, 3771−3776.
(39) Fauziah, C. A.; Al-yaseri, A. Z.; Beloborodov, R.; Siddiqui, M. A. Q.; Lebedev, M.; Parsons, D.; Roshan, H.; Barifcani, A.; Iglauer, S. Carbon dioxide/brine, nitrogen/brine, and oil/brine wettability of montmorillonite, Illite, and kaolinite at elevated pressure and temperature. *Energy Fuels* **2019**, *33*, 441.
(40) Myshakin, E. M.; Saidi, W. A.; Romanov, V. N.; Cygan, R. T.; Jordan, K. D. Molecular dynamics simulations of carbon dioxide interaction in hydrated Na-montmorillonite. *J. Phys. Chem. C* **2013**, *117* (21), 11028−11039.
(41) Šolc, R.; Gerzabek, M. H.; Lischka, H.; Tunega, D. Wetatbility of kaolinite (001) surfaces − Molecular dynamic study. *Geoderma* **2011**, *169*, 47−54.
(42) Roshan, H.; Ehsani, S.; Marjo, C. E.; Andersen, M. S.; Acworth, R. I. Mechanisms of water adsorption into partially saturated fractured shales: An experimental study. *Fuel* **2015**, *159*, 628−637.

DOI: 10.1021/acs.energyfuels.8b03536
Energy Fuels 2019, 33, 788−795

(43) Arif, M.; Lebedev, M.; Barifcani, A.; Iglauer, S. Influence of shale-total organic content on CO_2 geo-storage potential. *Geophys. Res. Lett.* **2017**, *44* (17), 8769−8775.
(44) Sang, Q.; Li, Y. J.; Yang, Z. H.; Zhu, C. F.; Yao, J.; Dong, M. Z. Experimental investigation of gas production processes in shale. *Int. J. Coal Geol.* **2016**, *159*, 30−47.
(45) Sang, Q.; Li, Y. J.; Zhu, C. F.; Zhang, S. J.; Dong, M. Z. Experimental investigation of shale gas production with different pressure depletion schemes. *Fuel* **2016**, *186*, 293−304.
(46) Espinoza, D. N.; Santamarina, J. C. CO_2 breakthrough − Caprock sealing efficiency and integrity for carbon geological storage. *Int. J. Greenhouse Gas Control* **2017**, *66*, 218−229.
(47) Shojai Kaveh, N.; Wolf, K.-H.; Barnhoorn, A. Wettability evaluation of silty shale caprocks for CO_2 storage. *Int. J. Greenhouse Gas Control* **2016**, *49*, 425−435.
(48) Love, J. C.; Estroff, L. A.; Kriebel, J. K.; Nuzzo, R. G.; Whitesides, G. M. Self-assembled monolayers of thiolates on metals as a form of nanotechnology. *Chem. Rev.* **2005**, *105* (4), 1103−1169.
(49) Iglauer, S.; Salamah, A.; Sarmadivaleh, M.; Liu, K. Y.; Phan, C. Contamination of silica surfaces: Impact on water−CO_2−quartz and glass contact angle measurements. *Int. J. Greenhouse Gas Control* **2014**, *22*, 325−328.
(50) Song, W.; Kovscek, A. R. Functionalization of micromodels with kaolinite for investigation of low salinity oil-recovery processes. *Lab Chip* **2015**, *15*, 3314−3325.
(51) Rao, S. M.; Thyagaraj, T. Swell−compression behaviour of compacted clays under chemical gradients. *Can. Geotech. J.* **2007**, *44* (5), 520−532.
(52) Al-Yaseri, A. Z.; Lebedev, M.; Barifcani, A.; Iglauer, S. Receding and advancing (CO_2+ brine+ quartz) contact angles as a function of pressure, temperature, surface roughness, salt type and salinity. *J. Chem. Thermodyn.* **2016**, *93*, 416−423.
(53) Lander, L. M.; Siewierski, L. M.; Brittain, W. J.; Vogler, E. A. A systematic comparison of contact angle methods. *Langmuir* **1993**, *9* (8), 2237−2239.
(54) Zhang, Y. Q.; Sanati-Nezhad, A.; Hejazi, S. H. Geo-material surface modification of microchips using layer-by-layer (LbL) assembly for subsurface energy and environmental applications. *Lab Chip* **2018**, *18*, 285−295.
(55) Wang, L.-K.; Chen, G. J.; Han, G. H.; Guo, X. Q.; Guo, T. M. Experimental study on the solubility of natural gas components in water with or without hydrate inhibitor. *Fluid Phase Equilib.* **2003**, *207* (1−2), 143−154.
(56) Swanson, B. F. Rationalizing the influence of crude oil wetting on reservoir fluid flow with electrical resistivity behavior. *JPT, J. Pet. Technol.* **1980**, *32*, 1459.
(57) Pan, B.; Li, Y. J.; Xie, L. J.; Wang, X. P.; He, Q. K.; Li, Y. C.; Hejazi, S. H.; Iglauer, S. Role of fluid density on quartz wettability. *J. Pet. Sci. Eng.* **2019**, *172*, 511−516.
(58) Arif, M.; Al-Yaseri, A. Z.; Barifcani, A.; Lebedev, M.; Iglauer, S. Impact of pressure and temperature on CO_2−brine−mica contact angles and CO_2−brine interfacial tension: Implications for carbon geo-sequestration. *J. Colloid Interface Sci.* **2016**, *462*, 208−215.
(59) Arif, M.; Barifcani, A.; Lebedev, M.; Iglauer, S. Structural trapping capacity of oil-wet caprock as a function of pressure, temperature and salinity. *Int. J. Greenhouse Gas Control* **2016**, *50*, 112−120.
(60) Iglauer, S.; Mathew, M. S.; Bresme, F. Molecular dynamics computations of brine−CO_2 interfacial tensions and brine−CO_2−quartz contact angles and their effects on structural and residual trapping mechanisms in carbon geo-sequestration. *J. Colloid Interface Sci.* **2012**, *386* (1), 405−414.
(61) Iglauer, S. CO_2-water-rock wettability: Variability, influencing factors, and implications for CO_2 geostorage. *Acc. Chem. Res.* **2017**, *50* (5), 1134−1142.
(62) Chen, C.; Wan, J. M.; Li, W. Z.; Song, Y. C. Water contact angles on quartz surfaces under supercritical CO_2 sequestration conditions: Experimental and molecular dynamics simulation studies. *Int. J. Greenhouse Gas Control* **2015**, *42*, 655−665.
(63) Liang, Y. F.; Tsuji, S.; Jia, J. H.; Tsuji, T.; Matsuoka, T. Modeling CO_2−water−mineral wettability and mineralization for carbon geosequestration. *Acc. Chem. Res.* **2017**, *50*, 1530−1540.
(64) Arif, M.; Barifcani, A.; Iglauer, S. Solid/CO_2 and solid/water interfacial tensions as a function of pressure, temperature, salinity and mineral type: Implications for CO_2-wettability and CO_2 geo-storage. *Int. J. Greenhouse Gas Control* **2016**, *53*, 263−273.
(65) Liu, Y. L.; Li, H. Z.; Okuno, R. Measurements and modeling of interfacial tension for CO_2/CH_4/brine systems under reservoir conditions. *Ind. Eng. Chem. Res.* **2016**, *55* (48), 12358−12375.
(66) Pinon, A. V.; Wierez-Kien, M.; Craciun, A. D.; Beyer, N.; Gallani, J. L.; Rastei, M. V. Thermal effects on van der Waals adhesive forces. *Phys. Rev. B: Condens. Matter Mater. Phys.* **2016**, *93* (3), 035424.
(67) Sayyouh, M. H.; Dahab, A. S.; Omar, A. E. Effect of clay content on wettability of sandstone reservoirs. *J. Pet. Sci. Eng.* **1990**, *4* (2), 119−125.
(68) Lebedeva, E. V.; Fogden, A. Micro-CT and wettability analysis of oil recovery from sand packs and the effect of waterflood salinity and kaolinite. *Energy Fuels* **2011**, *25* (12), 5683−5694.
(69) Lebedeva, E. V.; Fogden, A. Adhesion of oil to kaolinite in water. *Environ. Sci. Technol.* **2010**, *44* (24), 9470−9475.
(70) Chiquet, P.; Broseta, D.; Thibeau, S. Wettability alteration of caprock minerals by carbon dioxide. *Geofluids* **2007**, *7*, 112−122.
(71) Arif, M.; Jones, F.; Barifcani, A.; Iglauer, S. Electrochemical investigation of the effect of temperature, salinity, and salt type on brine/mineral interfacial properties. *Int. J. Greenhouse Gas Control* **2017**, *59*, 136−147.
(72) Vane, L. M.; Zang, G. M. Effect of aqueous phase properties on clay particle zeta potential and electro-osmotic permeability: Implications for electro-kinetic soil remediation processes. *J. Hazard. Mater.* **1997**, *55*, 1−22.
(73) Cagnola, A.; Li, Z.; Roshan, H.; Masoumi, H. Microstructural Evolution of Organic Matter-Rich Shales by Ionic Solutions. In Proceedings of the *51st U.S. Rock Mechanics/Geomechanics Symposium*, 25−28 June, San Francisco, California, USA; American Rock Mechanics Association: 2017, https://www.onepetro.org/conference-paper/ARMA-2017-0138.
(74) Rezaei Gomari, K. A.; Hamouda, A. A. Effect of fatty acids, water composition and pH on the wettability alteration of calcite surface. *J. Pet. Sci. Eng.* **2006**, *50* (2), 140−150.
(75) Alipour Tabrizy, V.; Denoyel, R.; Hamouda, A. A. Characterization of wettability alteration of calcite, quartz and kaolinite: Surface energy analysis. *Colloids Surf., A* **2011**, *384*, 98−108.
(76) Dlapa, P.; Doerr, S. H.; Lichner, L.; Šír, M.; Tesař, M. Effect of kaolinite and Ca-montmorillonite on the alleviation of soil water repellency. *Plant, Soil Environ.* **2011**, *50* (8), 358−363.
(77) Iglauer, S.; Lebedev, M. High pressure-elevated temperature x-ray micro-computed tomography for subsurface applications. *Adv. Colloid Interface Sci.* **2018**, *256*, 393.
(78) Tombácz, E.; Szekeres, M. Surface charge heterogeneity of kaolinite in aqueous suspension in comparison with montmorillonite. *Appl. Clay Sci.* **2006**, *34*, 105−124.
(79) Wan, J. M.; Tokunaga, T. K. Partitioning of clay colloids at air-water interfaces. *J. Colloid Interface Sci.* **2002**, *247* (1), 54−61.

DOI: 10.1021/acs.energyfuels.8b03536
Energy Fuels 2019, 33, 788−795